Self-Assembly of Designed Antimicrobial Peptides in Solution and Micelles[†]

Maryam M. Javadpour and Mary D. Barkley*,[‡]

Departments of Chemistry and Biochemistry, Louisiana State University, Baton Rouge, Louisiana 70803

Received July 8, 1996; Revised Manuscript Received May 29, 1997[⊗]

ABSTRACT: Hydrophobic interactions are responsible for stabilizing leucine zippers in peptides containing heptad repeats. The effects of substituting leucine by phenylalanine and alanine by glycine on the self-assembly of coiled-coils were examined in minimalist antimicrobial peptides designed to form amphipathic α-helices. The secondary structure of these peptides was monitored in solution and in diphosphocholine (DPC) micelles using circular dichroism spectroscopy. The leucine peptides $(KLAKLAK)_3$ and $(KLAKKLA)_n$ ($n = 3, 4$) become α-helical with increasing concentrations of salt, peptide, and DPC. The aggregation state and equilibrium constant for self-association of the peptides were measured by sedimentation equilibrium. The glycine peptide $(KLGKKLG)_3$ does not self-associate. The leucine peptides and phenylalanine peptides $(KFAKFAK)_3$ and $(KFAKKFA)_n$ ($n = 3, 4$) are in a monomer−tetramer equilibrium in solution, with the phenylalanine zippers being 2−4 kcal/mol less stable than the equivalent leucine zippers. Thermodynamic parameters for the association reaction were calculated from the temperature dependence of the association constants. Leucine zipper formation has $\Delta C_p = 0$, whereas phenylalanine zipper formation has a small negative ΔC_p, presumably due to the removal of the larger surface area of phenylalanine from water. Self-association of the peptides is coupled to formation of a hydrophobic core as detected using 1-anilino-naphthalene-8-sulfonate fluorescence. Carboxyfluorescein-labeled peptides were used to determine the aggregation state of $(KLAKKLA)_3$ and $(KLGKKLG)_3$ in DPC micelles. $(KLAKKLA)_3$ forms dimers, and $(KLGKKLG)_3$ is a monomer. Aggregation appears to correlate with the cytotoxicity of these peptides.

Amphipathic α-helices have opposing polar and nonpolar faces oriented along the helix axis. These helices make up 50% of the α-helices found in soluble globular proteins (*1*, *2*). They also occur in DNA-binding proteins (*3*, *4*), fibrous proteins (*5*−*7*), and smaller polypeptides such as hormones (*8*, *9*) and venoms (*9*, *10*). Recently, it has become apparent that many organisms, ranging from prokaryotes to humans, use amphipathic peptides as part of their host defense system (*11*−*13*). These antimicrobial peptides kill bacteria and other pathogens by disrupting the cell membrane.

The coiled-coil is a widespread structural motif consisting of two to four α-helices characterized by a heptad repeat of seven amino acids designated a through g (*14*). This structure features a hydrophobic interface between the amphipathic helices of the coiled-coil. Most heptad repeats use leucines at positions a and d to form the hydrophobic face of the helix. Positions e and g are often charged residues (*7*) whose side chains can also participate in interhelical electrostatic interactions (*15*, *16*), whereas positions b, c, and f are generally exterior residues exposed to solvent. Coiled-coils with as few as 14 residues (GAL4−DNA complex; *17*) and as many as 1086 residues (myosin; *18*) occur in proteins. In a number of proteins of diverse function (*7*, *19*), the coiled-coil domain has been identified as the noncovalent dimerization surface for homodimer (*20*) and heterodimer assembly (*4*). However, the majority of studies investigating the factors that contribute to the formation and stability of coiled-coils use synthetic peptides of *de novo* design containing 5−7 hydrophobic heptad repeats (*21*, *22*). Recently Su et al. (*23*) reported that a minimum of three heptads corresponding to six helical turns is required for a peptide to adopt a two-stranded α-helical coiled-coil conformation in aqueous solution.

Amphipathic α-helices have a pronounced tendency to self-associate. The equilibrium constant for self-association of amphipathic peptides results from two antagonistic effects: a favorable hydrophobic effect that leads to burial of nonpolar residues within the oligomer, and an unfavorable electrostatic force due to proximity of highly charged surfaces. Self-association is promoted by screening the charges and also by increasing the size of the nonpolar face in the peptides. Synthetic helices have been designed that aggregate to form dimers, trimers, tetramers, and hexamers with parallel and antiparallel orientations (*24*−*28*). Substitution of different hydrophobic residues at position a opposite leucine residues at position d of the heptad repeat demonstrated the importance of hydrophobic interactions on the self-association and stability of amphipathic α-helices (*29*). Sedimentation equilibrium experiments showed that synthetic 21-mer peptides having valine or leucine residues at position a form tetramers with the leucine−leucine interactions being 4 kcal mol^{-1} more stable than valine−leucine interactions. Peptides with alanine or threonine residues at position a failed to associate even at high peptide concentrations. Electrostatic interactions between ion-pairs at positions b and c of the heptad repeat are also responsible for self-association of peptides (*30*). The oligomerization state of synthetic peptides

[†] This work was supported by NSF/EPSCoR Grant (RII/ EPSCoR)-LEQSF(1992-96)-ADP-01. The analytical ultracentrifuge was purchased with NSF Grant BIR-9420253 and Grant LEQSF-ENH-TR-59 from the State of Louisiana.

* Address correspondence to this author.

[‡] Present address: Department of Chemistry, Case Western Reserve University, 10900 Euclid Ave., Cleveland, OH 44106-7078. E-mail: mdb4@po.cwru.edu.

[⊗] Abstract published in *Advance ACS Abstracts,* July 15, 1997.

S0006-2960(96)01644-3 CCC: $14.00

containing either glutamic acid or lysine residues at positions b and c of the tetramerization domain of Lac repressor was determined by sedimentation equilibrium. The Lac21E and Lac21K peptides were monomeric, whereas the Lac21E/Lac21K peptide mixture formed heterotetramers.

Using a minimalist approach (*31*, *32*), we previously designed amphipathic α-helical peptides with heptad repeats that have high antimicrobial activity (*33*). In this paper, we examine the self-association of these and other related peptides. We investigate the effects of the size of the nonpolar domain and of substitution of phenylalanine at positions a and d on the stability and aggregation state of the coiled-coil in solution. Circular dichroism spectroscopy is used to monitor peptide secondary structure. Analytical ultracentrifugation is used to determine the oligomerization model and equilibrium constant. Thermodynamic properties of the self-association are derived from the temperature dependence of the equilibrium constant. We also determine the aggregation state of carboxyfluorescein-labeled peptides in dodecylphosphocholine (DPC)[1] micelles. Finally, the effect of self-assembly on the antimicrobial activity of the peptides is considered.

MATERIALS AND METHODS

Peptide Synthesis and Labeling. The peptides were synthesized by a solid-phase method using a MilliGen 9050 PepSynthesizer. 9-Fluorenylmethyloxycarbonyl amino acids protected at the α-amino function were purchased from MilliGen (Burlington, MA), and activated as pentafluorophenyl esters at the carboxyl function. Coupling was performed using HOBt (Fisher Biotech, Fair Lawn, NJ) in an extended cycle. Polystyrene resin with a peptide amide linker was purchased from MilliGen. The peptide was cleaved from the resin and deprotected by treatment with trifluoroacetic acid reagent (88% TFA, 5% water, 5% phenol, 2% triisopropylsilane) for 2−4 h, extracted in cold 20% acetic acid and diethyl ether, and lyophilized.

Peptides were purified by reversed-phase chromatography on a Waters 15 μ Deltapak C_4 column (200 × 25 mm) using a gradient of 10−50% acetonitrile (0.05% v/v TFA) and water (0.05% v/v TFA). Purity was checked on an analytical Vydac 5 μ C_{18} column monitored with a UV detector at 220 nm. The molecular mass of purified peptide was verified by plasma desorption mass spectrometry. Peptides were stored as lyophilized powders at −20 °C. Peptide concentrations were determined by quantitative amino acid analysis. Peptide samples containing a norleucine standard were hydrolyzed in 6 N HCl, 0.1% phenol, for 24 h at 110 °C, followed by sodium cation exchange chromatography on a Pickering column (3 × 250 mm) and detection of the amino acid by reaction with ninhydrin at 130 °C.

Peptides were labeled at their N-termini with carboxyfluorescein (Eastman Kodak, Rochester, NY). Derivatization was carried out on the resin using the following coupling cycle: 1 mol equiv each of carboxyfluorescein, BOP (Castro's reagent; Millipore, Bedford, MA), and HOBt and 1.5 mol equiv of NMM in dry DMF for 3−5 h. Peptides were cleaved from the resin, deprotected, and purified by HPLC as described above. Fluorescent-labeled peptides were monitored during HPLC using UV (220 nm) and fluorescence (excitation 470 nm, emission 520 nm) detectors. The correct product was confirmed by plasma desorption mass spectrometry, and peptide concentration was determined by quantitative amino acid analysis.

Circular Dichroism. CD measurements were made using an Aviv 60DS spectropolarimeter. The calibration was checked with (+)-10-camphorsulfonic acid (Sigma, St. Louis, MO) (*34*). All CD spectra were recorded from 250 to 190 nm in quartz cells of 0.1−0.001 cm path length at room temperature with 1-nm bandwidth, 10-nm/min scan speed, and 5-s time constant. Duplicate scans were acquired to improve the signal-to-noise ratio. A base line was recorded and subtracted after each spectrum. The mean residue ellipticity, $[\theta]$ in deg cm^2 dmol^{-1}, was calculated from

$$[\theta] = [\theta]_{obs}(\mathrm{MRW}/10lc) \quad (1)$$

where $[\theta]_{obs}$ is the ellipticity measured in millidegrees, MRW is the mean residue molecular mass of the peptide (molecular mass divided by the number of amino acid residues), l is the optical path length of the cell in centimeters, and c is the concentration of the sample in milligrams per milliliter. Since all the peptides were synthesized as C-terminal amides, the C-terminus acts as an extra residue (W. C. Johnson, personal communication). Percent α-helix was determined from the molar ellipticity measured at 222 nm $[\theta]_{222}$ using

$$\%\ \alpha\text{-helix} = ([\theta]_{222} \times 100)/[-40000(1 - 2.5/n)] \quad (2)$$

where n is the number of amino acid residues in the peptide (*35*).

Analytical Ultracentrifugation. Sedimentation equilibrium experiments were performed using a Beckman XL-A analytical ultracentrifuge. Experiments were run in a 4-hole rotor with a counterbalance and 3 carbon-filled epoxy double-sector cells at a rotor speed of 40 000 rpm at 10 temperatures from 2 to 38 °C. Peptides were dissolved in 2.5 mM sodium phosphate buffer, pH 7.4, 0.4 M NaCl. Peptide concentrations were 1 and 2 mM for 21-mer leucine peptides, 2 and 4 mM for 21-mer phenylalanine peptides, and 0.1 mM for 28-mer peptides. The concentration distribution of peptide within the cell was determined by the absorbance at 254 or 236 nm for the 21- or 28-mer leucine peptides and at 273 or 222 nm for the 21- or 28-mer phenylalanine peptides. Base line scans were measured at 365 nm, where the peptides have no absorption. The time required to attain equilibrium at the first temperature was established by running until the scans were invariant for 12 h; this was achieved by 34 h. The temperature was increased in 4 °C increments, and scans were taken after 24 h at each temperature. This time was sufficient for reequilibration at the new temperature. Scans were collected with a radial step size of 0.001; 10 acquisitions were averaged at each radial position to give the final data for analysis.

Concentration distributions were fit to various mathematical models by least squares using MLAB [Civilized Software, Inc., Bethesda, MD (*36*)]. Best fit criteria were minimum sum of squares of the residuals, random distribution of the residuals, and minimum standard errors of parameters. The mathematical model for a reversible monomer−tetramer

[1] Abbreviations: ANS, 1-anilinonaphthalene-8-sulfonate; BOP, benzotriazol-1-yloxytris(dimethylamino)phosphonium hexafluorophosphate; CD, circular dichroism; CF, carboxyfluorescein; DMF, *N*,*N*′-dimethylformamide; DPC, dodecylphosphocholine; HOBt, 1-hydroxybenzotriazole; MEM, minimal essential medium; MIC, minimum inhibitory concentration; NMM, *N*-methylmorpholine; TFA, trifluoroacetic acid; Tris, tris(hydroxymethyl)aminomethane.

interaction is

$$c_r = c_{b,1} \exp[AM_1(r^2 - r_b^2)] + c_{b,1}^4 \exp[\ln k_{14} + 4AM_1(r^2 - r_b^2)] + \epsilon \quad (3)$$

where $c_{b,1}$ is the concentration of monomer at r_b, the radial position of the cell bottom; M_1 is the molecular mass of the monomer calculated from the amino acid sequence; and ϵ is a small base-line error correction term. $A = (1 - \bar{v}\rho)\omega^2/2RT$, where $\bar{v}$ is the partial specific volume of the monomer, ρ is solvent density, ω is angular velocity, R is the gas constant, and T is absolute temperature. The partial specific volume of the monomer was calculated from the amino acid sequence of the peptide (*37*), and was corrected for temperature (*38*): 0.783 ± 0.005 for $(KFAKKFA)_3$, $(KFAKFAK)_3$, and $(KFAKKFA)_4$; 0.824 ± 0.005 for $(KLAKKLA)_3$ and $(KLAKLAK)_3$; 0.804 ± 0.005 for $(KLGKKLG)_3$; 0.818 ± 0.005 for $(KLAKKLA)_4$. A partial specific volume of 0.789 ± 0.003 was measured for $(KLAKKLA)_3$ using H_2O- and D_2O-containing buffers (*39*). The molecular mass was adjusted for the H−D exchange, and the two sedimentation equilibrium data sets were fitted simultaneously to eq 3 with $\bar{v}$ as an adjustable parameter. Equation 3 assumes that monomer and tetramer have the same partial specific volume. The equilibrium constant for tetramer formation is defined as $k_{14} = c_{b,4}/c_{b,1}^4$, where $c_{b,1}$ and $c_{b,4}$ refer to the concentration of monomer and tetramer, respectively, at the radial position of the cell bottom and are given in terms of the absorbance at the scanning wavelength. If the tetramer species is absent, the data analysis will return a large negative number for the value of ln k_{14}.

The use of the logarithm of the equilibrium constant in eq 3 acts as an implicit constraint by ensuring that the equilibrium constants have positive values. Fitting for ln k_{14} also has the advantage that the logarithm of the molar equilibrium constant, taking 1 mol of the monomer as the standard state, is given by $\ln K_{14} = \ln k_{14} + \ln (E_1^3/4)$ where E_1 is the molar extinction coefficient of the monomer at the scanning wavelength. The ln K_{14} values are used to calculate thermodynamic parameters such as the standard free energy change, $\Delta G^\circ = -RT \ln K$. Finally, the standard error estimates for fits to the logarithm of the equilibrium constant appear to be more nearly valid (*40*).

The temperature dependence of ln K_{14} was analyzed by the method of Clarke and Glew (*41*) using the Taylor's series expansion about the reference temperature θ:

$$R \ln K = -\Delta G^\circ_\theta/\theta + \Delta H^\circ_\theta(1/\theta - 1/T) + \Delta C^\circ_{p,\theta}[\theta/T - 1 + \ln (T/\theta)] + \theta/2(d\Delta C^\circ_p/dT)_\theta[(T/\theta) - (\theta/T) - 2\ln(T/\theta)] + \theta^2/12(d^2\Delta C^\circ_p/dT^2)_\theta[(T/\theta)^2 - 6(T/\theta) + 3 + 2(\theta/T) + 6\ln (T/\theta)] \quad (4)$$

Equation 4 describes the temperature dependence of the equilibrium constant. The fitting parameters are the changes in free energy (ΔG°_θ), enthalpy (ΔH°_θ), heat capacity at constant pressure ($\Delta C^\circ_{p,\theta}$), and first and second temperature derivatives of the heat capacity change, ($d\Delta C^\circ_p/dT$ and $d^2\Delta C^\circ_p/dT^2$). The reference temperature was taken to be 298.15 K. Data were weighted by the normalized reciprocals of the variances of the values of ln k calculated from the approximate standard errors obtained when fitting the sedimentation equilibrium concentration distribution. Best fit criteria were minimum sum of squares and minimum standard errors of parameters.

The molecular mass of peptides in micelles was measured at 22 °C by the method of Reynolds and Tanford (*42*). Samples were made from stock solutions of DPC and carboxyfluorescein-labeled peptide diluted to the final concentration with different ratios of H_2O/D_2O to yield a range of densities. Stock solutions were 0.3 M DPC in 25 mM sodium phosphate buffer, 0.1 M NaCl, pH 7.4; 0.01 M CF-$(KLAKKLA)_3$ in water; and 0.01 M CF-$(KLGKKLG)_3$ in water. Final concentrations were 2.5 mM sodium phosphate buffer, pH 7.4, 0.01 M NaCl containing 2×10^{-4} M CF-peptide and 3×10^{-2} M DPC. This DPC concentration was >20-fold above the critical micelle concentration of 1.1×10^{-3} M (*43*). Reference solutions contained 3×10^{-2} M DPC and buffer at the same density as the sample. Densities ranging from 0.99905 to 1.09236 g/cm^3 were measured on a Paar DMA 58 density meter. Concentration distributions of carboxyfluorescein-labeled peptides within the cell were determined from the absorbance at 537 nm. Base line scans were measured at 634 nm, where the labeled peptide and detergent have no absorbance. The time required to reach equilibrium was 34 h. Partial specific volumes of carboxyfluorescein-labeled peptides in solution were measured as described above: 0.741 ± 0.005 for CF-$(KLAKKLA)_3$ and 0.777 ± 0.002 for CF-$(KLGKKLG)_3$.

Fluorescence Quantum Yields. Quantum yields were determined relative to ANS in ethanol on an SLM 8000 spectrofluorometer interfaced to a Macintosh IIcx computer. Samples contained $(2-4) \times 10^{-3}$ M peptide, 1×10^{-5} M ANS in 2.5 mM sodium phosphate buffer, pH 7.4, 0.4 M NaCl. All peptides except $(KLGKLGK)_3$ and $(KKAKKKA)_3$ are tetrameric under these conditions as shown by circular dichroism and sedimentation equilibrium. Temperature was maintained at 25 °C with a Lauda circulating bath. Samples were excited at 360 nm, and emission spectra were scanned from 410 to 600 nm in the ratio mode with single excitation and emission monochromators set at 4- and 8-nm band-pass, respectively. Magic angle polarizers were set to 55° on the excitation side and 0° on the emission side to avoid the Wood's anomaly of the emission grating. A solvent blank was subtracted, and spectra were corrected for wavelength-dependent instrument response using correction factors determined with a standard lamp from Optronics.

Biological Activity. MICs of peptides were determined against *Escherichia coli* ATCC 25922, *Pseudomonas aeraginosa* ATCC 27853, and *Staphylococcus aureus* ATCC 25723. *E. coli* and *P. aeraginosa* are Gram-negative bacteria; *S. aureus* is a Gram-positive bacterium. Peptide 1:2 serial dilutions were prepared from 512 μg/mL stock solutions to give a range of 256−2 μg/mL in the culture media. Bacterial cultures were grown to mid-log phase in nutrient broth and were standardized to a 0.5 McFarland turbidity tube before dilution. An equal volume of peptide solution was added to each sterile well containing 5×10^4 cells in 50 μL. The MIC is the lowest peptide concentration that inhibits cell growth as evidenced by absence of turbidity after 4 h (*44*). The median assay values are reported for 3−7 separate tests. Assay results vary by no more than one dilution from the median value.

The efficacy of peptides in killing 3T3 mouse fibroblasts was determined by a 2-fold serial dilution assay. Fifty microliters of a stock peptide solution was diluted with an equal volume of MEM, and 1:2 serial dilutions in MEM

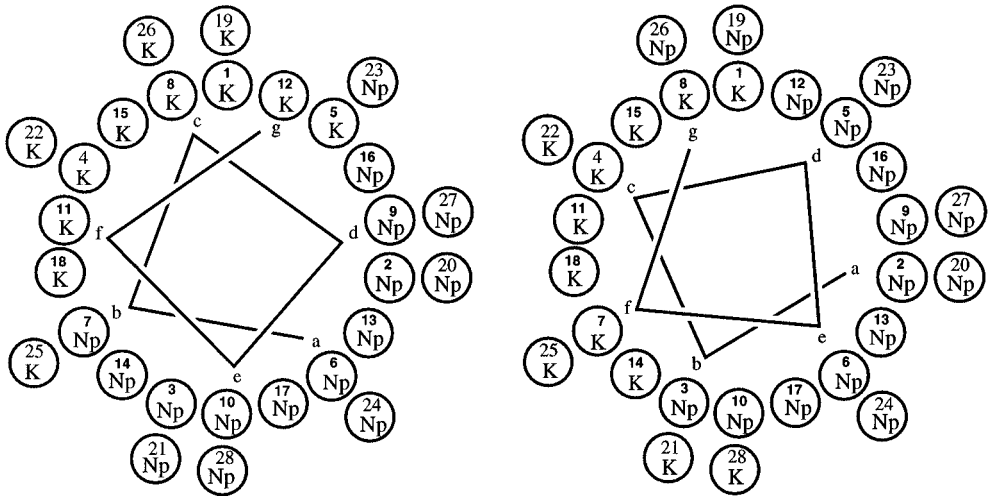

FIGURE 1: Wheel diagram of the designed peptides with the general sequences (left) $[(KNpNp)K(KNpNp)]_4$ and (right) $[(KNpNp)(KNpNp)K]_4$.

were prepared. Each dilution was applied to a 1-day-old monolayer of 3T3 cells (approximately 1×10^4 cells/well) maintained in a 96-well plate with fresh MEM (50 μL/well). Peptide-treated and peptide-free control cells were incubated at 37 °C for 30 min. The supernatant was removed, and the cells were gently treated with 0.2% trypan blue stain and viewed in an inverted light microscope. Inclusion of trypan blue dye within a cell is indicative of cell death. A sublethal dose is defined as the highest dilution in which only 1−10 adherent cells are not stained.

RESULTS

Peptide Design. Peptides with the general sequences $[(KNpNp)(KNpNp)K]_n$ and $[(KNpNp)K(KNpNp)]_n$, where the nonpolar residues Np = A/G and L/F and $n = 3$ and 4, were designed to form amphipathic α-helices (Figure 1). These sequences are isomeric, differing only in the position of the initial residue of the heptad repeat. In general, most designed amphipathic helices use alanine and leucine residues to form the hydrophobic face of the helix. These residues have high helix propensity (*45*−*47*). Lysine is chosen as the polar residue not only because of high helix propensity (*7*), but also because the presence of lysine and alanine on adjacent turns of the helix stabilizes the coiled-coil (*48*). The leucine peptides have the sequences $(KLAKLAK)_3$ and $(KLAKKLA)_n$, while the phenylalanine peptides substitute phenylalanine for leucine, $(KFAKFAK)_3$ and $(KFAKKFA)_n$. Since the hydrophobicities of leucine and phenylalanine appear to be the same (*49*, *50*), these peptides probe the effect of side chain shape at positions a and d on the stability and number of strands in the coiled-coil. A peptide substituting glycine for alanine, $(KLGKKLG)_3$, was also synthesized. Glycine is a helix-destabilizing amino acid (*51*−*54*).

Secondary Structure. Circular dichroism spectroscopy was used to monitor the secondary structure of the peptides. CD spectra were measured in two buffers at 25 °C: 2.5 mM sodium phosphate buffer, pH 7.4, or 10 mM Tris buffer, pH 7.4. The 21-mer peptides have a random structure with a characteristic minimum near 200 nm in both buffers. The 28-mer peptides form large insoluble aggregates in phosphate buffer. However, the 28-mers are soluble in Tris buffer with ∼41% α-helix. The designed amphipathic α-helices have a polar face consisting entirely of lysines with a total charge of +9 and +12, respectively, for the 21- and 28-mer peptides. Repulsive forces between the charged lysines favor the extended random structure. According to polyelectrolyte theory, increasing the salt concentration should promote α-helix formation by screening the positive charges of the lysines (*55*). The CD spectra of the peptides were recorded as a function of NaCl concentration from 0 to 1 M at constant peptide concentration. All of the peptides except $(KLGKKLG)_3$ become more α-helical with increasing NaCl concentration in both phosphate and Tris buffers. Their CD spectra are characteristic of an α-helix with a distinct minimum at 222 nm (n−π* transition), a second minimum close to 208 nm (superposition of the random coil π−π* transition at 200 nm and the α-helix π−π* transition at 208 nm), and the α-helix maximum at 193 nm. An isodichroic point is observed at 203 nm, indicating a local two-state equilibrium with each residue in either helical or random-coil conformation (*56*). The salt dependence of the molar ellipticity at 222 nm is shown in Figure 2. The extent of helix formation of the peptides appears to be independent of buffer. The 28-mers are more helical at lower salt concentrations than the 21-mers, suggesting a larger contribution from the nonelectrostatic component of the free energy of helix formation.

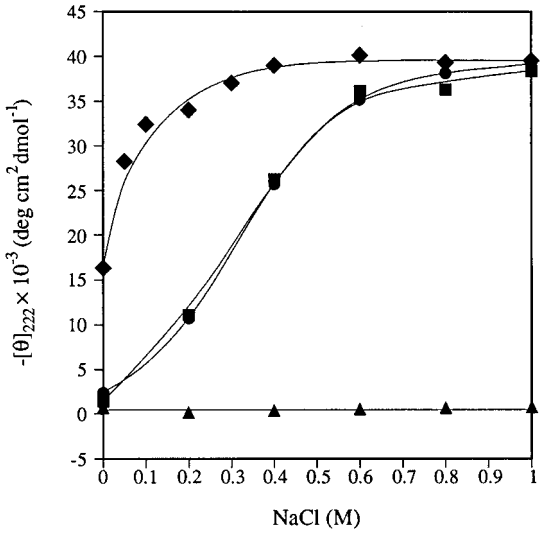

FIGURE 2: Molar ellipticity of peptides at 222 nm as a function of NaCl concentration. Peptide concentration is 6.4×10^{-4} M. (▲) $(KLGKKLG)_3$ and (●) $(KLAKKLA)_3$ in 2.5 mM sodium phosphate buffer, pH 7.4; (◆) $(KLAKKLA)_4$ and (■) $(KLAKKLA)_3$ in 10 mM Tris buffer, pH 7.4. Lines drawn to guide the eye.

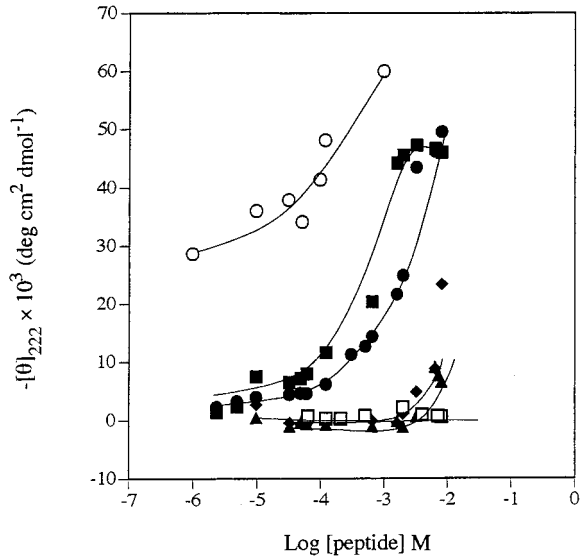

FIGURE 3: Molar ellipticity of peptides at 222 nm as a function of peptide concentration. 2.5 mM phosphate buffer, pH 7.4, 0.4 M NaCl. (●) $(KLAKKLA)_3$, (■) $(KLAKLAK)_3$, (◆) $(KFAKFAK)_3$, (▲) $(KFAKKFA)_3$, (○) $(KLAKKLA)_4$, and (□) $(KLGKKLG)_3$. Lines drawn to guide the eye.

Helix formation is coupled to aggregation in peptides with heptad repeats. An aggregation-induced increase in helicity with increasing peptide concentration is detected by circular dichroism (*23*, *57*, *58*). To determine if the salt-dependent helical form of the 21- and 28-mer peptides is oligomeric, the concentration dependence of the CD spectra was determined in 2.5 mM phosphate buffer, pH 7.4, 0.4 M NaCl at 25 °C. The molar ellipticity of these peptides depends on concentration, showing that helix formation is accompanied by self-association (Figure 3). The driving force for self-assembly is the association of hydrophobic side chains (*59*). In $(KLAKLAK)_n$ and $(KLAKKLA)_n$, ($n = 3$, 4), the hydrophobic leucine residues are presumed to form the intermolecular interface, while in $(KFAKFAK)_n$ and $(KFAKKFA)_n$ ($n = 3$, 4), the phenylalanine residues would be at the interface. The 28-mer peptides self-associate at concentrations as low as 1 μM. The extra heptad is responsible for the higher helical content of the 28-mer peptides relative to the 21-mers. Even though helices 21−28 residues in length are sufficient to form coiled-coils, an increase in the size of the hydrophobic segment results in greater stability of interchain hydrophobic interactions (*23*, *24*, *60*). The aromatic residues of phenylalanine induce positive CD signals causing significant errors in the estimation of the helical content from the ellipticity values at 222 nm (*61*, *62*). Therefore, the extent of helix formation in the leucine and phenylalanine peptides cannot be directly compared. However, our main interest here is the concentration dependence of the CD. In contrast to the other designed peptides, $(KLGKKLG)_3$ shows no salt- or concentration-dependent changes in the CD spectrum. $(KLGKKLG)_3$ has two glycines per heptad at position b in the polar face and position e on the nonpolar face of the amphipathic helix. This implies that the intermolecular hydrophobic interactions are not strong enough to compensate for the helix destabilization of the glycine residues in the 21-mer peptide. However, longer peptides 29−35 residues in length having a single glycine at either position b or position f in the polar face of the heptad repeat form stable coiled-coils (*24*, *63*).

The carboxyfluorescein-labeled peptides also have random-coil conformation in 2.5 mM phosphate buffer, pH 7.4, 0.01 M NaCl. Association of the peptides with DPC micelles induces α-helical secondary structure. CD spectra of CF-$(KLAKKLA)_3$ and CF-$(KLGKKLG)_3$ were measured as a function of DPC concentration by increasing the detergent:peptide ratio from 0 to 500:1. Isodichroic points were observed at 203 nm, indicating a local two-state equilibrium between random coil and α-helical conformations (Figure 4, upper panel). Minimum molar ellipticity at 222 nm was reached for CF-$(KLAKKLA)_3$ and CF-$(KLGKKLG)_3$ at detergent:peptide ratios of 50:1 and 125:1, respectively (Figure 4, lower panel). The helix contents of detergent-bound CF-$(KLAKKLA)_3$ and CF-$(KLGKKLG)_3$ are 85% and 46%. These values are close to the helix contents of 88% and 48% obtained for unlabeled $(KLAKKLA)_3$ and $(KLGKKLG)_3$ in DPC micelles (not shown).

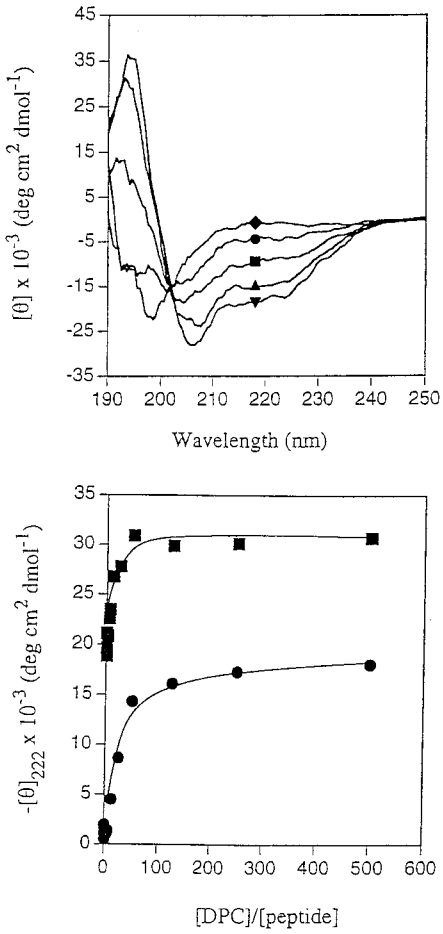

FIGURE 4: Upper panel: circular dichroism spectra of 2×10^{-4} M CF-$(KLGKKLG)_3$ as a function of DPC concentration. (◆) 0 mM, (●) 2.5 mM, (■) 5 mM, (▲) 10 mM, and (▼) 100 mM. Isodichroic point at 203 nm. Lower panel: molar ellipticity of (●) CF-$(KLGKKLG)_3$ and (■) CF-$(KLAKKLA)_3$ at 222 nm as a function of DPC concentration. Peptide concentration is 2×10^{-4} M. Lines drawn to guide the eye.

Self-Assembly in Solution. Sedimentation equilibrium was used to examine the association state of the peptides in aqueous solution and to measure the related association constants. Experiments were performed as a function of temperature at 4 C° intervals from 2 to 38 °C. The data were fit to various models for the self-assembly, assuming the same partial specific volume for all species. The partial specific volume of $(KLAKKLA)_3$ measured in the ultracentrifuge (*39*) agrees well with the value calculated from the amino acid sequence of the peptide (*37*). This confirms that the partial specific volume of the peptides does not vary with association state. It also indicates that the volume change

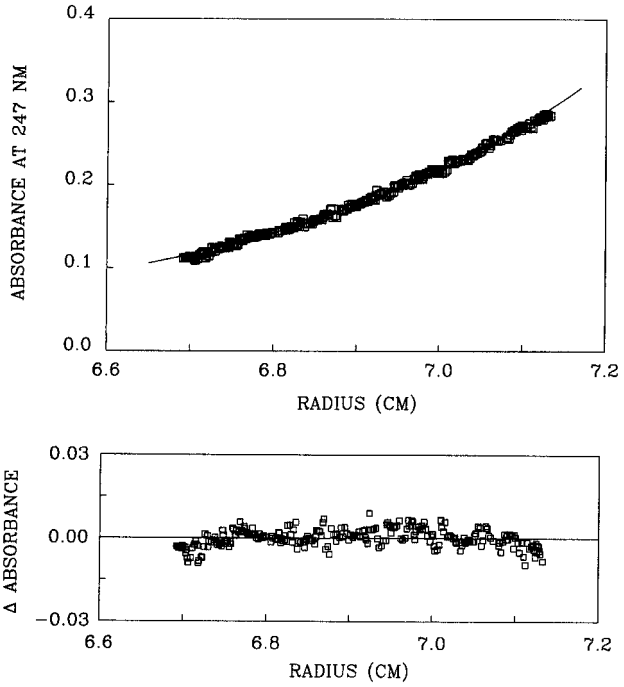

FIGURE 5: Sedimentation equilibrium of $(KLGKKLG)_3$ at 26 °C. Upper panel: concentration distribution of 4 mM $(KLGKKLG)_3$ in 2.5 mM phosphate buffer, pH 7.4, 0.4 M NaCl. The line is the best fit for the monomer model. Lower panel: residuals for the fit.

$dV = 0$ for the association reaction, so that the value of the association constant is not perturbed by sedimentation in the XL-A ultracentrifuge. The parameters $\ln k_{14}$, $c_{b,1}$, and ϵ were treated as adjustable parameters in the data analysis. A, M_1, and r_b were fixed at their known values. To ensure correct models for the association reaction and accurate values for the association constants, some of the peptides were run at two different concentrations, and the data were analyzed simultaneously in a global fit. $(KLGKKLG)_3$ is monomeric at all temperatures (Figure 5). The rest of the peptides are in a monomer−tetramer equilibrium (Figure 6). During the analysis, $M_1 \leftrightarrow M_2$ and $M_1 \leftrightarrow M_2 \leftrightarrow M_4$ were also considered as possible models. However, the fits for $M_1 \leftrightarrow M_2$ were poor (Figure 6). The fits for $M_1 \leftrightarrow M_2 \leftrightarrow M_4$ were much better than for the $M_1 \leftrightarrow M_2$ model, but gave either very small values of $\ln k_{12}$ or worse fits than the $M_1 \leftrightarrow M_4$ model. Moreover, the temperature dependence of the equilibrium constants was poorly behaved for the $M_1 \leftrightarrow M_2 \leftrightarrow M_4$ model. Thus, while we cannot completely eliminate the possibility that the peptides may dimerize as well, the dimer concentration appears to be too low to resolve two equilibrium constants. Models for $M_1 \leftrightarrow M_3$, $M_1 \leftrightarrow M_6$, and $M_1 \leftrightarrow M_8$ were also considered, but negative values of $\ln k$ or positive values with unacceptable errors were obtained.

Equation 4 was used to determine the thermodynamic parameters from the temperature dependence of $R \ln K$. In the Clark and Glew method, the data are fit by including successively higher order terms in the Taylor expansion. For the leucine peptides $(KLAKLAK)_3$ and $(KLAKKLA)_n$ ($n = 3, 4$), the best fit was obtained with terms for ΔG°_θ and ΔH°_θ . Adding the term for $\Delta C^\circ_{p,\theta}$ increased the sum of squares of the fit 2-fold, so $\Delta C^\circ_{p,\theta}$ was set to zero. This means that the value of ΔC°_p over the temperature range studied is very small. On the other hand, for the phenylalanine peptides $(KFAKFAK)_3$ and $(KFAKKFA)_n$ ($n = 3, 4$), the $\Delta C^\circ_{p,\theta}$, $(d\Delta C^\circ_p/dT)_\theta$, and $(d^2\Delta C^\circ_p/dT^2)_\theta$ terms were necessary for a good fit. We also included the next higher

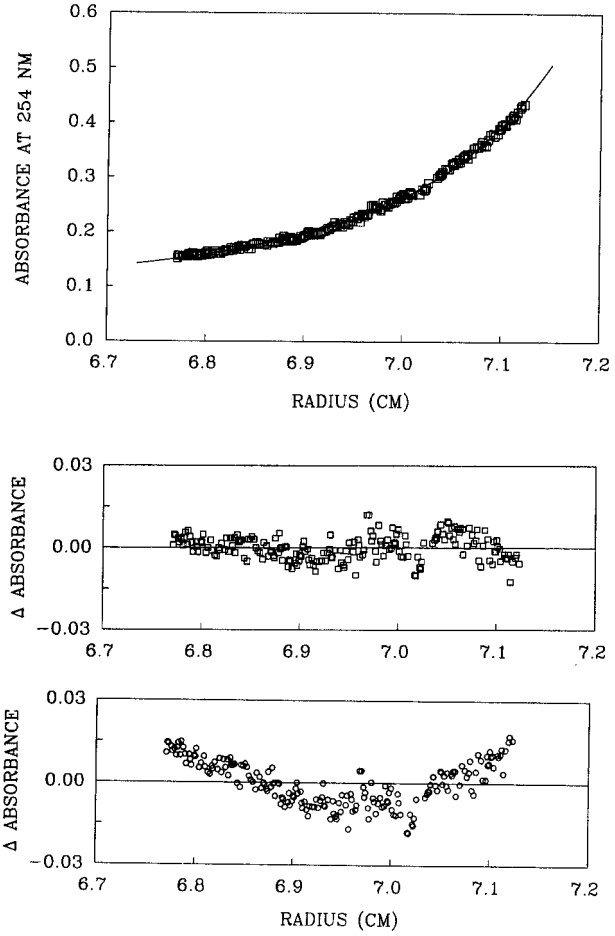

FIGURE 6: Sedimentation equilibrium of $(KLAKKLA)_3$ at 26 °C. Upper panel: concentration distribution of 2 mM $(KLAKKLA)_3$ in 2.5 mM phosphate buffer, pH 7.4, 0.4 M NaCl. The line is the best fit for the monomer−tetramer equilibrium model. Middle panel: residuals for fit to monomer−tetramer equilibrium. Lower panel: residuals for fit to monomer−dimer equilibrium.

term $(d^3\Delta C^\circ_p/dT^3)_\theta$ in the fit, but this increased the errors indicating $(d^3\Delta C^\circ_p/dT^3)_\theta = 0$. The nonzero values for $(d\Delta C^\circ_p/dT)_\theta$ and $(d^2\Delta C^\circ_p/dT^2)_\theta$ mean that ΔC°_p is a parabolic function of temperature T. Figure 7 plots $\Delta G^\circ = -RT \ln K$ as a function of temperature. The curvature of the plot for the phenylalanine peptides clearly demonstrates that ΔC°_p is nonzero, whereas the straight line for the leucine peptides indicates that ΔH and ΔS are independent of temperature. Table 1 contains the derived thermodynamic parameters of the peptides at 25 °C.

Self-Assembly in Micelles. According to the CD spectra, the designed peptides adopt α-helical conformations in solution and in DPC micelles. We have just shown that α-helix formation in solution is coupled to self-association to the tetramer. The method of Reynolds and Tanford (*42*) was used to determine the aggregation state of CF-$(KLAKKLA)_3$ and CF-$(KLGKKLG)_3$ bound to DPC micelles by sedimentation equilibrium. Briefly, at a solvent density matching the detergent density, the apparent molecular weight of the peptide−DPC complex becomes equal to the molecular weight of the protein component. At this density, the detergent does not contribute to the sedimentation potential of the complex. If the chemical potential of all solvent components is kept constant, the experimentally observed concentration gradient is a measure of $M_p(1 - \phi'\rho)$, where M_p is the molecular mass of the peptide moiety in the sedimenting particle, ρ is the solvent density, and ϕ' is

Table 1: Thermodynamic Parameters for Monomer−Tetramer Equilibrium at $\theta = 298.15$ K[a]

peptide	$\Delta G°_\theta$ (kcal/mol)	$\Delta H°_\theta$ (kcal/mol)	$\Delta S°_\theta$ [cal/(mol· deg)]	$\Delta C°_{p,\theta}$ [kcal/(mol· deg)]	$(\Delta C°_p/dT)_\theta$ [kcal/(mol·deg^2)]	$(d^2\Delta C°_p/dT^2)_\theta$ [kcal/(mol·deg^3)]
$(KFAKKFA)_3$	-9.6 ± 0.1	-22.0 ± 4.7	-41.6 ± 8.9	-2.8 ± 0.2	-0.1 ± 0.1	0.02 ± 0.03
$(KFAKFAK)_3$	-10.4 ± 0.01	-22.9 ± 1.6	-42.0 ± 3.0	-1.6 ± 0.2	0.2 ± 0.1	0.04 ± 0.01
$(KLAKKLA)_3$	-11.5 ± 0.1	-6.5 ± 2.0	16.9 ± 5.2	0	0	0
$(KLAKLAK)_3$	-12.1 ± 0.1	-4.0 ± 1.4	27.0 ± 9.5	0	0	0
$(KFAKKFA)_4$	-20.0 ± 0.2	-26.8 ± 9.0	-24.1 ± 8.1	-1.2 ± 0.9	0.04 ± 0.3	-0.001 ± 0.06
$(KLAKKLA)_4$	-23.6 ± 0.2	27.0 ± 5.0	170 ± 31.5	0	0	0
CF-$(KLAKKLA)_3$	-6.8 ± 0.2					

[a] 2.5 mM sodium phosphate buffer, pH 7.4, 0.4 M NaCl.

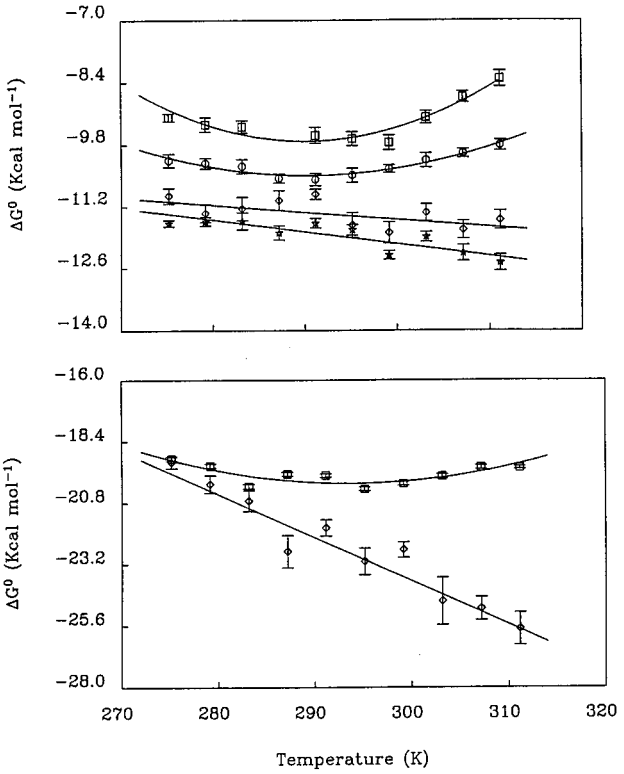

FIGURE 7: Temperature dependence of free energy for monomer−tetramer equilibrium. Error bars are standard errors obtained from fits of equilibrium concentration distributions. Lines are best fits to eq 4. Upper panel: (□) $(KFAKKFA)_3$, (○) $(KFAKFAK)_3$, (◇) $(KLAKKLA)_3$, and (★) $(KLAKLAK)_3$. Lower panel: (□) $(KFAKKFA)_4$ and (◇) $(KLAKKLA)_4$.

the volume increment per gram of peptide. Since the measurement of ϕ' is difficult $M_p(1 - \phi'\rho)$ is expressed in terms of the individual contributions in the sedimenting particle.

$$M_p(1 - \phi'\rho) = M_p[(1 - \bar{v}_p\rho) + \delta_D(1 - \bar{v}_D\rho)] \quad (5)$$

where $\bar{v}_p$ is the partial specific volume of the peptide, $\bar{v}_D$ is the partial specific volume of the detergent, and δ_D is the grams of detergent in the sedimenting particle. At $\rho = 1/\bar{v}_D$, the detergent term vanishes, $1 - \bar{v}_D\rho = 0$, and

$$M_p(1 - \phi'\rho) = M_p[(1 - \bar{v}_p\rho)] \quad (6)$$

This condition is attained by adjusting the density with D_2O.

Our experiments take advantage of an optical probe covalently bound to the peptides. By monitoring wavelengths where only carboxyfluorescein absorbs, the concentration distribution of the peptide can be determined without background absorption from the detergent. Figure 8 plots the apparent value of $M_p(1 - \phi'\rho)$ for CF-$(KLAKKLA)_3$ and CF-$(KLGKKLG)_3$ as a function of solvent density. DPC

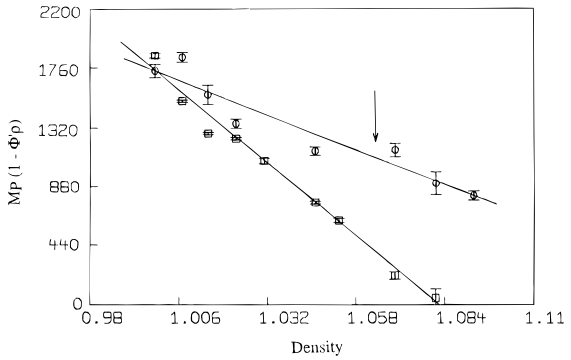

FIGURE 8: Sedimentation equilibrium of (○) CF-$(KLGKKLG)_3$ and (□) CF-$(KLAKKLA)_3$ in DPC micelles by the method of Reynolds and Tanford (1976). $M_p(1 - \phi'\rho)$ is plotted versus solvent density, ρ, which is varied by mixing different proportions of H_2O and D_2O buffers. Lines are least-squares fits to data. Arrow indicates the solvent density for which $\rho = 1/\bar{v}$ of DPC.

has a partial specific volume of 0.937 cm^3/g (*43*). The molecular masses are obtained from eq 6 at $\rho = 1/\bar{v}_D$. The monomer molecular masses of CF-$(KLAKKLA)_3$ and CF-$(KLGKKLG)_3$ are 2634 and 2562, respectively. The sedimentation equilibrium values of 5050 ± 80 and 1870 ± 70 for CF-$(KLAKKLA)_3$ and CF-$(KLGKKLG)_3$ measured in DPC micelles correspond to dimers and monomers, respectively.

ANS Fluorescence. ANS is a hydrophobic fluorescent probe, whose fluorescence intensity increases and emission spectrum shifts to shorter wavelengths in nonpolar environments (*64*, *65*). It is practically nonfluorescent in water. As seen in Figure 9, the fluorescence of ANS increases in the presence of the self-associating peptides, indicative of binding to a hydrophobic environment. The quantum yields of the peptide−ANS complex were measured relative to ANS in ethanol. The quantum yield is 2−3-fold higher for ANS bound to phenylalanine peptides than to leucine peptides: 0.189 and 0.276 for $(KFAKFAK)_3$ and $(KFAKKFA)_3$, compared to 0.066 and 0.126 for $(KLAKLAK)_3$ and $(KLAKKLA)_3$, respectively. These results suggest that the designed amphipathic peptides aggregate through the association of their hydrophobic side chains to form a hydrophobic core. The fluorescence of ANS only increases slightly in the presence of $(KLGKKLG)_3$ with a quantum yield of 0.024. This peptide does not self-associate. The slight increase in ANS fluorescence could be due to interaction of the probe with the hydrophobic leucine residues. In the presence of a control peptide $(KKAKKKA)_3$ lacking the leucine residues, the quantum yield of ANS is 0.01, which is the same as the value in buffer.

Biological Activity. The designed peptides were tested against Gram-negative and Gram-positive bacteria and also against mammalian cells (Table 2). Data for three naturally

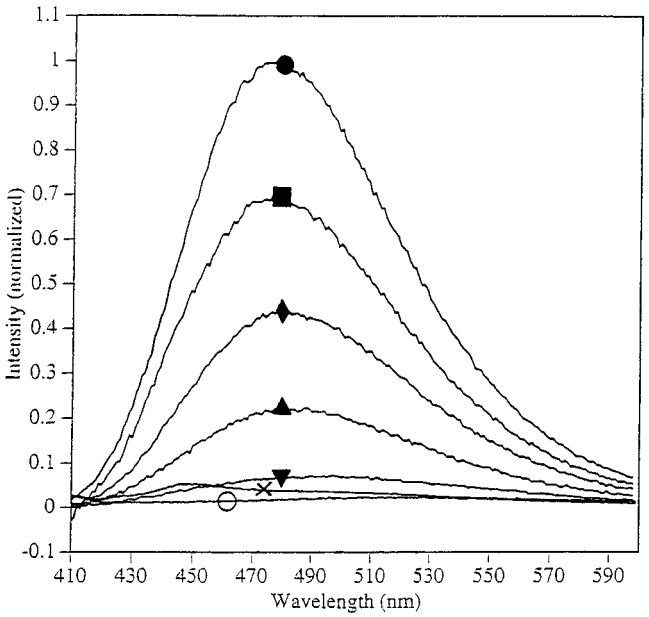

FIGURE 9: Emission spectra of 1×10^{-5} M ANS in the presence of 2×10^{-3} M peptide. Top to bottom: (●) $(KFAKKFA)_3$, (■) $(KFAKFAK)_3$, (◆) $(KLAKKLA)_3$, (▲) $(KLAKLAK)_3$, (▼) $(KLGKKLG)_3$, (×) $(KKAKKKA)_3$, and (○) 2.5 mM phosphate buffer, pH 7.4, 0.4 M NaCl.

Table 2: Biological Activity of Designed Peptides

peptide	MIC μM			3T3 μM
	E. coli	*P. aeruginosa*	*S. aureus*	
$(KLGKKLG)_3$[a]	4	4	4	>393
$(KLAKKLA)_3$[a]	4	4	4	11
$(KLAKLAK)_3$[a]	4	4	4	9
$(KFAKKFA)_3$	2	4	3	5
$(KFAKFAK)_3$	3	4	3	11
$(KLAKKLA)_4$	9	9	9	10
$(KFAKKFA)_4$[b]	–	–	–	4
CF-$(KLAKKLA)_3$	6		6	
CF-$(KLGKKLG)_3$	6		3	
melittin[a]	3	6	3	1
magainin 2 amide[a]	10	5	19	60
cecropin B amide[a]	1		12	102

[a] Data from ref. 33. [b] Peptide precipitated in MIC assay mixture.

occurring antimicrobial peptides, magainin 2 amide, cecropin B amide, and melittin, are included for comparison (*33*). Melittin is a hemolytic peptide from bee venom, which also has antimicrobial activity [for review, see ref *66*). The magainins and cecropins are families of antimicrobial peptides that act only on bacteria (*11*, *67*). The MIC assay measures inhibition of bacterial cell growth. The designed peptides and melittin all have the same antimicrobial activity within one dilution toward Gram-positive and Gram-negative bacteria, whereas magainin 2 and cecropin B are much less potent toward Gram-positive bacteria. The mammalian cell assay determines the efficacy of peptides to induce cell death in 3T3 mouse fibroblasts. The most dramatic difference in cytotoxicity of the designed peptides is exhibited by $(KLGKKLG)_3$. In killing 3T3 cells, this peptide is about 40 times less potent compared to the designed peptides and melittin, but 7 and 4 times less potent compared to magainin 2 and cecropin B, respectively. The carboxyfluorescein-labeled peptides have the same biological activity, within experimental error, as their equivalent unlabeled peptides.

DISCUSSION

Among the different types of noncovalent interactions in polypeptides and proteins, hydrophobic interactions between nonpolar residues are thought to be one of the most important in forming and stabilizing the native protein structure (*68*, *69*). The nature of the hydrophobic interactions depends on solvent environment. In this paper, we have demonstrated that phenylalanine interactions stabilize the self-association of cationic peptides. These phenylalanine interactions are 2−4 kcal/mol less stable than the equivalent leucine interactions in the presence of 0.4 M NaCl. The aromatic residues may restrict the side-chain conformation and thereby destabilize the α-helix.

All of the designed peptides except for $(KLGKKLG)_3$ associate to form tetramers in 2.5 mM phosphate buffer, 0.4 M NaCl, pH 7.4. Unlike the amphipathic alanine-based peptides 16−17 residues in length that form monomeric helices (*70*, *71*), $(KLGKKLG)_3$ is a random coil in aqueous solution. Apparently, the intermolecular hydrophobic interactions are not strong enough to compensate for the helix destabilization of the six glycine residues in this peptide, and consequently no conformational transition occurs in solution at high peptide or salt concentration. The designed peptides that do self-associate have α-helical conformations in solution. The phenylalanine peptides $(KFAKFAK)_3$ and $(KFAKKFA)_3$ are capable of self-associating; however, their CD spectra have relatively small negative ellipticities at 222 nm; the percent helicities calculated from eq 2 are 3% and 0%, respectively. Assuming that the tetramer is 100% helical, we can estimate the helix content from the equilibrium constants for self-assembly: 20% and 7% for $(KFAKFAK)_3$ and $(KFAKKFA)_3$. The lower helix contents derived from circular dichroism may be due to the positive signals induced by the phenylalanine residues (*62*). On the other hand, circular dichroism overestimates the helix contents of the leucine peptides $(KLAKLAK)_3$ and $(KLAKKLA)_3$: 133% and 122%, respectively, compared to only 49% and 43% calculated from the association constants. Two possible reasons for a higher helix content estimated by circular dichroism are as follows: (1) monomeric helices in equilibrium with tetramer or (2) anomalously large negative ellipticities of nonrandom helical aggregates (*72*, *73*). Molar ellipticities at 222 nm with magnitudes as large as 60 000 are seen in the concentration studies of these peptides (Figure 3).

The aggregation state and helicity of the peptides are environmentally sensitive. In aqueous solution, all the peptides, except $(KLGKKLG)_3$, form tetrameric helical bundles; in hexafluoroisopropyl alcohol, they form octameric bundles (*74*). In DPC micelles, CF-$(KLAKKLA)_3$ exists as a dimer, and CF-$(KLGKKLG)_3$ is a monomer. The carboxyfluorescein label does not affect the aggregation state. In the presence of micelles, CF-$(KLAKKLA)_3$ has a helix content of 85% compared to 88% for the unlabeled peptide. CF-$(KLGKKLG)_3$ is 46% α-helix, and the unlabeled peptide is 48%. These values compare to 90% helical content for $(KLAKKLA)_3$ and 63% for $(KLGKKLG)_3$ when bound to neutral vesicles (*75*).

The thermodynamic parameters quantify the self-assembly of the designed peptides. The 21-mer peptides with the general sequence of $[(KNpNp)(KNpNp)K]_3$ are ~0.6 kcal/mol more stable compared to $[(KNpNp)K(KNpNp)]_3$. The coiled-coil starts at residue 2 in the former peptides and at

residue 6 in the latter peptides. Attachment of carboxyfluorescein to the N-terminus of $(KLAKKLA)_3$ has no effect on aggregation state, but destabilizes the tetramer by ~4 kcal/mol. Tetramer formation in the 28-mer peptides is more stable compared to the 21-mer peptides by ~11.0 kcal/mol. This can be attributed to the additional heptad repeat present in the 28-mer peptides. An increase in the length of the nonpolar domain does not affect the aggregation state of the peptides, but it provides a larger region of hydrophobic interactions and thus additional stability. For the leucine peptides, $\Delta C°_{p,\theta} = 0$ and the temperature melts are noncooperative (data not shown). However, the curvature in the plot of $\Delta G°$ as a function of temperature and the negative value of $\Delta C°_{p,\theta}$ for the phenylalanine peptides resemble the behavior of natural proteins. Negative $\Delta C°_{p,\theta}$ values result from withdrawal of nonpolar groups from the aqueous environment (*76*, *77*). The difference in the $\Delta C°_{p,\theta}$ values of the leucine and phenyalanine peptides can be attributed to the relative size of the water-accessible nonpolar surface area of leucine and phenylalanine residues. Since leucine has a smaller nonpolar surface area compared to phenylalanine (*77*), the $\Delta C°_{p,\theta}$ value may be too small to be measured accurately over the narrow temperature range studied.

The signs and magnitudes of the $\Delta H°$ and $\Delta S°$ values for the association reactions of the designed peptides can be attributed to the strength and extent of the hydrophobic interactions between the nonpolar residues. Ross and Subramanian (*78*) envision peptide association as a two-step process proceeding from isolated hydrated species to a partially interacting state with mutual penetration of hydration layers, and from there to an association complex. Positive enthalpy and entropy changes occur in the first step as a result of partial withdrawal of the nonpolar groups from water accompanied by an increase in the number of unstructured water molecules (*78*−*80*). Negative enthalpy and entropy changes arise in the second step from short-range noncovalent interactions such as strengthened van der Waals interactions and hydrogen-bond formation (*13* , *43*, *78*−*80*). Since the hydrophobicities of leucine and phenylalanine are about the same (*49*, *50*), association of the leucine and phenylalanine peptides should give approximately the same positive values for $\Delta H°$ and $\Delta S°$. However, phenylalanine has a larger nonpolar surface area than leucine (*77*), so that the overall values of $\Delta H°$ and $\Delta S°$ are more negative due to stronger van der Waals interactions in the phenylalanine peptides. This is consistent with the greater increase in quantum yield of the ANS complexes with phenylalanine peptides compared to leucine peptides. Computer modeling suggests that the bulky aromatic rings of the phenylalanine residues form a larger hydrophobic core that is more accessible to ANS.

Structure−function correlation in antibacterial peptides is a subject of intensive research due to the emergence of antibiotic-resistant pathogenic microorganisms (*81*, *82*). The correlation between the biological activity of designed peptides and their propensity to adopt an α-helical conformation is well established (*33*, *83*). Bishop et al. (*75*) have studied the interaction of $(KLGKKLG)_3$ and $(KLAKKLA)_3$ with model membranes. Their results suggest that the helix propensity of the peptides in a membrane environment is an important factor in the binding affinity, which correlates with biological activity. They and others (*84*) showed that amphipathic peptides with high helical content disrupt lipid vesicles. However, the role of self-association of the amphipathic peptides was unclear. In the present study, all the peptides inhibited bacterial growth to the same extent based on the MICs. However, unlike the other designed peptides, $(KLGKKLG)_3$ is very selective in discriminating between bacterial and mammalian cells. $(KLGKKLG)_3$ then behaves similarly to the magainins (*85*) and cecropins (*86*), which are monomeric antimicrobial peptides with low cytotoxicity to mammalian cells. The other peptides are like melittin, which forms a tetramer in solution and kills mammalian cells (*87*). These correlations suggest that aggregation plays a role in the selectivity of antimicrobial peptides. Thus, it appears that the mechanisms of toxicity differ in bacterial and mammalian cells with cytotoxicity in mammalian cells requiring self-association of the peptide.

ACKNOWLEDGMENT

We are grateful to Dr. Marc S. Lewis for help with analytical ultracentrifugation and analysis of association reactions and for critical reading of the manuscript. Sedimentation equilibrium experiments on $(KFAKKFA)_3$ and $(KFAKFAK)_3$ were performed in the National Center for Research Resources at NIH, Bethesda, MD. We thank Ms. Martha M. Juban for peptide synthesis and bioassays, and Dr. Steven M. Bishop for labeled peptides.

REFERENCES

1. Cornette, J. L., Cease, K. B., Margalit, H., Spouge, J. L., Berzofsky, J. A., and De Lisi, C. D. (1987) *J. Mol. Biol. 195*, 659.
2. Segrest, J. P., De Loof, H., Dohlman, J. G., Brouillette, C. G., and Anantharamaiah, G. M. (1990) *Proteins*: *Struct., Funct., Genet. 8*, 103−117.
3. Landschulz, W. H., Johnson, P. F., and McKnight, S. L. (1988) *Science 240*, 1759−1764.
4. O'Shea, E. K., Rutkowski, R., and Kim, P. S. (1989) *Science 243*, 538−542.
5. Sodek, J., Hodges, R. S., Smillie, L. B., and Jurasek, L. (1972) *Proc. Natl. Acad. Sci. U.S.A. 69*, 3800−3804.
6. Hodges, R. S., Saund, A. K., Chong, P. C. S., St.-Pierre, S. A., and Reid, R. E. (1981) *J. Biol. Chem. 256*, 1214−1221.
7. Cohen, C., and Parry, D. A. D. (1986) *Trends Biochem. Sci. 11*, 245−248.
8. Kaiser, E. T., and Kezdy, F. J. (1983) *Proc. Natl. Acad. Sci. U.S.A. 80*, 1137−1143.
9. Taylor, J., Osterman, D. G., Miller, R. J., and Kaiser, E. T. (1984) *J. Am. Chem. Soc. 103*, 6965−6966.
10. Argiolas, A., and Pisano, T. J. (1985) *J. Biol. Chem. 260*, 1437.
11. Zasloff, M. (1987) *Proc. Natl. Acad. Sci. U.S.A. 84*, 5449−5453.
12. Boman, H. G., and Hultmark, D. (1987) *Annu. Rev. Microbiol. 41*, 103−126.
13. Ganz, T., Selsted, M. E., and Lehrer, R. I. (1990) *Eur. J. Hemotol. 44*, 1−8.
14. McLachlan, A. D., and Stewart, M. (1975) *J. Mol. Biol. 98*, 293−304.
15. Lumb, K. J., and Kim, P. S. (1995) *Science 268*, 436−439.
16. Glover, J. N. M., and Harrison, S. C. (1995) *Nature 373*, 257−261.
17. Marmorstein, R., Carey, M., Ptashne, M., and Harrison, S. C. (1992) *Nature 356*, 408−414.
18. McLachlan, A. D., and Karn, S. (1982) *Nature 299*, 226−231.
19. Lupas, A., Van Dyke, M., and Stock, J. (1991) *Science 252*, 1162−1164.
20. O'Shea, E. K., Rutkowski, R., and Kim, P. S. (1992) *Cell 68*, 699−708.
21. Monera, O. D., Zhou, N. E., Kay, C. M., and Hodges, R. S. (1993) *J. Biol. Chem. 268*, 19218−19227.
22. Thompson, K. S., Vinson, C. R., and Freire, E. (1993) *Biochemistry 32*, 5491−5496.

23. Su, J. Y., Hodges, R. S., and Kay, C. M. (1994) *Biochemistry 33*, 15501−15510.
24. Lau, S. M. Y., Taneja, A. K., and Hodges, R. S. (1984) *J. Biol. Chem. 259*, 13253−13261.
25. Regan, L., and DeGrado, W. F. (1988) *Science 241*, 976−978.
26. Hill, C. P., Anderson, D. H., Wesson, L., DeGrado, W. F., and Eisenberg, D. (1990) *Science 249*, 543−546.
27. Chin, T. M., Berndt, K. P., and Yang, N.-C. (1992) *J. Am. Chem. Soc. 114*, 2279−2280.
28. Harbury, P. B., Zhang, T., Kim, P. S., and Alber, T. (1993) *Science 262*, 1401−1407.
29. Betz, S. F., and DeGrado, W. F. (1996) *Biochemistry 35*, 6955−6962.
30. Fairman, R., Chao, H.-G., Lavoie, T. B., Villafranca, J. J., Matsueda, G. R., and Novotny, J. (1996) *Biochemistry 35*, 2824−2829.
31. Zhou, N. E., Zhou, B.-Y., Kay, C. M., and Hodges, R. S. (1992) *Biopolymers 32*, 419−426.
32. Åkerfeldt, K. S., Lear, J. D., Wassman, Z. R., Chung, L. A., and DeGrado, W. F. (1993) *Acc. Chem. Res. 26*, 191−197.
33. Javadpour, M. M., Juban, M. M., Lo, W.-C. J., Bishop, S. M., Alberty, J. B., Cowell, S. M., Becker, C. L., and McLaughlin, M. L. (1996) *J. Med. Chem. 39*, 3107−3113.
34. Chen, G. C., and Yang, J. T. (1977) *Anal. Lett. 10*, 1195−1207.
35. Chen, Y.-H., Yang, J. T., and Chau, K. H. (1974) *Biochemistry 13*, 3350−3359.
36. Knott, G. D. (1979) *Comput. Programs Biomed. 10*, 271−280.
37. Perkins, S. J. (1986) *Eur. J. Biochem. 157*, 169−180.
38. Durchschlog, H. (1986) *Thermodynamic Data for Biochemistry and Biotechnology*, Springer-Verlag, New York.
39. Edelstein, S. J., and Schachman, H. K. (1967) *J. Biol. Chem. 242*, 306−311.
40. Lewis, M. S. (1992) in *Analytical Ultracentrifugation in Biochemistry and Polymer Science* (Harding, S. E., Rowe, A. J., and Horton, J. C., Eds.) pp 126−137, Royal Society of Chemistry, Cambridge, England.
41. Clarke, E. C., and Glew, D. N. (1966) *Trans. Faraday Soc. 62*, 539−547.
42. Reynolds, J. A., and Tanford, C. (1976) *Proc. Natl. Acad. Sci. U.S.A. 73*, 4467−4470.
43. Lauterwein, J., Bosch, C., Brown, L. R., and Wuthrich, K. (1979) *Biochim. Biophys. Acta. 556*, 244−264.
44. Waitz, J. A., Doern, G. V., Finegold, S. M., Gavan, T. L., Hackett, J. L., Jones, R. N., Jorgensen, J. H., King, J. R., Miller, G. H., Reller, L. B., Thornsberry, C., Thrupp, L. D., and Zabransky, R. J. (1990) in *Methods for Dilution Antimicrobial Susceptibility Tests for Bacteria that Grow Aerobically, NCCLS Document M7-A2*, Vol. 10(8), pp 12−15, National Committee for Clinical Laboratory Standards, Villanova, PA.
45. Chou, P. Y., and Fasman, G. D. (1978) *Annu. Rev. Biochem. 47*, 251−276.
46. Scheraga, H. A. (1978) *Pure Appl. Chem. 50*, 315−324.
47. Sueki, M., Lee, S., Powers, S. P., Denton, J. B., Konishi, Y., and Scheraga, H. A. (1984) *Macromolecules 17*, 148−155.
48. Epand, R. M. (1993) *The Amphipathic Helix*, CRC Press, Boca Raton, FL.
49. Guo, D., Mant, C. T., Taneja, A. K., Parker, J. M. R., and Hodges, R. S. (1986) *J. Chromatogr. 359*, 499−517.
50. Parker, J. M. R., Guo, D., and Hodges, R. S. (1986) *Biochemistry 25*, 5425−5432.
51. Lyu, P. C., Liff, M. I., Marky, L. A., and Kallenbach, N. R. (1990) *Science 250*, 669−673.
52. O'Neil, K. T., and DeGrado, W. F. (1990) *Science 250*, 646−651.
53. Lyu, P. C., Wang, P. C., Liff, M. I., and Kallenbach, N. R. (1991) *J. Am. Chem. Soc. 113*, 3568−3572.
54. Chakrabartty, A., Kortemme, T., and Baldwin, R. L. (1994) *3*, 843−852.
55. Record, M. T., Jr., Anderson, C. F., and Lohman, T. M. (1978) *Q. Rev. Biophys. 11*, 103−178.
56. Holtzer, M. E., and Holtzer, A. (1995) *Biopolymers 36*, 365−379.
57. Osterhout, J. J., Jr., Handel, T., Na, G., Toumadje, A., Long, R. C., Connolly, P. J., Hoch, J. C., Johnson, W. C., Jr. , Live, D., and DeGrado, W. F. (1992) *J. Am. Chem. Soc. 114*, 331−337.
58. Lutgring, R., and Chmielewski, J. (1994) *J. Am. Chem. Soc. 116*, 6451−6452.
59. Bryson, J. W., Betz, S. F., Lu, H. S., Suich, D. J., Zhou, H. X., O'Neil, K. T., and DeGrado, W. F. (1995) *Science 270*, 935−941.
60. Lumb, K. J., Carr, C. M., and Kim, P. S. (1994) *Biochemistry 33*, 7361−7367.
61. Manning, M. C., and Woody, R. W. (1989) *Biochemistry 28*, 8609−8613.
62. Chakrabartty, A., Kortemme, T., Padmanabhan, S., and Baldwin, R. L. (1993) *Biochemistry 32*, 5560−5565.
63. Kohn, W. D., Kay, C. M., and Hodges, R. S. (1995) *Protein Sci. 4*, 237−250.
64. Slavik, J. (1982) *Biochim. Biophys. Acta. 694*, 1−25.
65. Semisotnov, G. V., Rodionova, N. A., Razgulyaev, O. I., Uversky, V. N., Gripas, A. F., and Gilmanshin, R. I. (1991) *Biopolymers 31*, 119−128.
66. Dempsey, C. E. (1990) *Biochim. Biophys. Acta 1031*, 143−161.
67. Boman, H. G., and Steiner, H. (1981) *Curr. Top. Microbiol. Immunol. 94*, 75−91.
68. DeGrado, W. F., and Lear, J. D. (1985) *J. Am. Chem. Soc. 107*, 7684−7689.
69. Muller, N. (1991) *Acc. Chem. Res 23*, 23−28.
70. Marqusee, S., and Baldwin, R. L. (1987) *Proc. Natl. Acad. Sci. U.S.A. 84*, 8898−8902.
71. Marqusee, S., Robbins, V. H., and Baldwin, R. L. (1989) *Proc. Natl. Acad. Sci. U.S.A. 86*, 5286−5290.
72. Keller, D., and Bustamante, C. (1986) *J. Chem. Phys. 84*, 2972−2980.
73. Kim, M.-H., Ulibarri, L., Keller, D., Maestre, M. F., and Bustamante, C. (1986) *J. Chem. Phys. 84*, 2981−2989.
74. Wang, X., Maskos, K., Javadpour, M. M., and Morden, K. M. (1997) *Biophys. J.* (manuscript in preparation).
75. Bishop, S. M., Smith-Wright, L., Tahir, J., Russo, P. S., and Barkley, M. D. (1997) *Biophys. J.* (in revision).
76. Spolar, R. S., Ha, J.-H., and Record, M. T., Jr. (1989) *Proc. Natl. Acad. Sci. U.S.A. 86*, 8382−8385.
77. Livingstone, J. R., Spolar, R. S., and Record, M. T., Jr. (1991) *Biochemistry 30*, 4237−4244.
78. Ross, P. D., and Subramanian, S. (1981) *Biochemistry 20*, 3096−3102.
79. Gill, S. J., Downing, M., and Sheats, G. F. (1967) *Biochemistry 6*, 272−276.
80. Gill, S. J., Nicholos, N. F., and Wadso, I. (1976) *J. Chem. Thermodyn. 8*, 445−452.
81. Neu, H. C. (1992) *Science 257*, 1064−1073.
82. Swartz, M. N. (1994) *Proc. Natl. Acad. Sci. U.S.A. 91*, 2420−2427.
83. Thennarasu, S., and Nagaraj, R. (1995) *Int. J. Pept. Protein Res. 46*, 480−486.
84. Dathe, M., Schümann, M., Wieprecht, T., Winkler, A., Beyermann, M., Krause, E., Matsuzaki, K., Murase, O., and Bienert, M. (1996) *Biochemistry 35*, 12612−12622.
85. Schümann, M., Dathe, M., Wieprect, T., Beyermann, M., and Bienert, M. (1997) *Biochemistry 36*, 4345−4351.
86. Gazit, E., Boman, A., Boman, H. G., and Shai, Y. (1995) *Biochemistry 34*, 11479−11488.
87. Wilcox, W., and Eisenberg, D. (1992) *Protein Sci. 1*, 641−653.

BI961644F